

tetraphenylboron gegenions are not intimately paired with the ammonium functional groups, one might expect that the Me-CD moieties would dissociate from the phenyl substituents of the porphyrin. Nevertheless, as assessed by TLC, the complex is stable in acetone and in 60% benzene/40% acetone (the latter is the eluent employed for the purification of **3**). We have recently demonstrated in a related system that a barrier does exist for the dissociation of the Me-CD moiety and that this barrier appears to be associated with solvation of the ammonium salt. Indeed, upon heating **3** to reflux in acetone, we begin to observe the formation of uncomplexed porphyrin. This process can be accelerated by treating the complex in acetone at room temperature with a trace of triethylamine.

The synthetic methodology described herein offers unusual flexibility in the construction of a range of heme-dependent protein mimics. Replacement of the Me-CD moieties with other hosts should provide a means to alter the size, shape, and hydrophobicity of the groove that circumscribes the porphyrin moiety. Since the groove has clear potential as a substrate binding site, such alterations may be useful in controlling substrate specificity. In addition, charged subunits of appropriate steric bulk can be used to covalently modify the primary amines of the porphyrin and thereby render the entire complex water soluble. These, as well as related studies, are currently in progress.

Acknowledgment. We thank Dr. Dinesh Sukumaran for helpful advice and Professor Dabney Dixon for bringing the paper cited in ref 9 to our attention. The National Science Foundation provided funds for the purchase of the NMR (CHE-8613066) and mass spectrometers (CHE-8509862) employed in this study. We thank the American Heart Association, National Center, for support of this research.

Supplementary Material Available: NMR data (^1H , ^{11}B , ^{13}C , ^{23}Na , NOE experiments), FAB MS data, combustion analysis, and the experimental protocol for compound **3** (1 page). Ordering information is given on any current masthead page.

(12) (a) Handy, P. R.; Popov, A. I. *Spectrochim. Acta* **1972**, *28A*, 1545. (b) Buxton, T. L.; Caruso, J. A. *J. Am. Chem. Soc.* **1974**, *96*, 6033. (c) Barker, B. J.; Sears, P. G. *J. Phys. Chem.* **1974**, *78*, 2687.

Dichloromethane: A Bridging Ligand

Mark Bown and Joyce M. Waters*

Department of Chemistry and Biochemistry
Massey University, Palmerston North, New Zealand

Received October 27, 1989

Recently, the first account of dichloromethane acting as a ligand was published.¹ We now report² a second example of the binding of this molecule to a metal. The compound $[(\eta^6\text{-C}_6\text{Me}_6)_2\text{Ru}_2\text{H}_2(\text{CH}_2\text{Cl}_2)]\text{RuB}_{10}\text{H}_8(\text{OEt})_2$ was prepared in 18% yield (based on Ru) by refluxing $[(\eta^6\text{-C}_6\text{Me}_6)_2\text{Ru}_2\text{H}_4]\text{RuB}_{10}\text{H}_8(\text{OEt})_2$ ⁴ and phenylacetylene in CH_2Cl_2 under an at-

(1) Newbound, T. D.; Colman, M. R.; Miller, M. M.; Wulfsberg, G. P.; Anderson, O. P.; Strauss, S. H. *J. Am. Chem. Soc.* **1989**, *111*, 3762.

(2) 1-(6',9'-Diethoxy-nido-octahydrodecaborato)-2,3-bis(η^6 -hexamethylbenzene)- μ_3 -hydrido-2,3- μ -hydrido-1,2- μ :1,3- μ -(dichloromethane)-triangulartriruthenium.

(3) Crystallographic data: Green crystal of $[(\eta^6\text{-C}_6\text{Me}_6)_2\text{Ru}_2\text{H}_2(\text{CH}_2\text{Cl}_2)]\text{RuB}_{10}\text{H}_8(\text{OEt})_2$, size $0.2 \times 0.2 \times 0.25$ mm, monoclinic $P2_1/n$, $a = 11.114$ (2) Å, $b = 17.748$ (3) Å, $c = 19.510$ (5) Å, $\beta = 103.18$ (2)°, $U = 3750$ (2) Å³, $Z = 4$, $T = 20$ °C, $D_{\text{calcd}} = 1.63$ g cm⁻³, $F(000) = 1856.0$, Enraf-Nonius CAD4 diffractometer, graphite monochromator, $\omega/2\theta$ scans, $\theta_{\text{max}} = 25$ °, 6553 unique data measured. Lorentz and polarization corrections, empirical absorption corrections, maximum and minimum values of 0.9992 and 0.9539 respectively, $\mu(\text{Mo K}\alpha) = 93.3$ cm⁻¹. Weighted least-squares refinement on F with neutral atom scattering factors and anomalous dispersion, anisotropic thermal parameters for all non-H atoms. Positional and thermal parameters refined for H atoms attached to B atoms and those associated with the Ru triangle; H atoms attached to C in fixed positions with $U = 0.05$ e Å⁻². $R = 0.040$, $R_w = 0.041$ for 488 variables and 3512 data for which $F^2 > 2.5\sigma(F^2)$; weight = $3.2739/(\sigma^2(F) + 0.000318F^2)$.

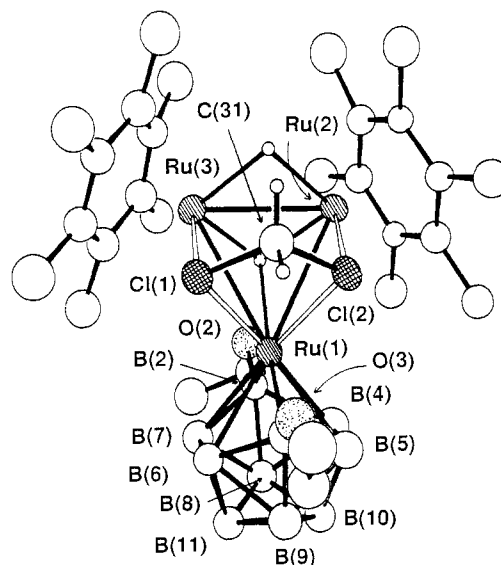


Figure 1. Diagram of the molecule $[(\eta^6\text{-C}_6\text{Me}_6)_2\text{Ru}_2\text{H}_2(\text{CH}_2\text{Cl}_2)]\text{RuB}_{10}\text{H}_8(\text{OEt})_2$. Thermal ellipsoids are drawn at the 50% probability level. Ru-C distances average at 2.24 Å; Ru-B distances lie in the range 2.10 (1)-2.36 (1) Å; other dimensions within the closo-type RuB_{10} cluster are similar to those already reported (ref 4). Proton and ^{11}B NMR data are as follows (ordered as $\delta(^{11}\text{B})/\text{ppm}$ (relative intensities in parentheses) [with directly bound $\delta(^1\text{H})/\text{ppm}$ in square brackets (relative intensities in parentheses)]): +99.0 (1 B) [OEt], +93.9 (1 B) [OEt], +1.4 (2 B) [+1.78 (2 H)], -1.3 (3 B) [+3.59 (1 H), +1.41 (2 H)], -4.0 (1 B) [+2.61 (1 H)], -6.5 (2 B) [+0.61 (2 H)]; also $\delta(^1\text{H})$ ($\eta^6\text{-C}_6\text{Me}_6$) +2.17 ppm; CD_2Cl_2 solution at 297 K.

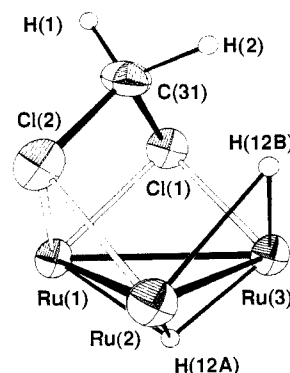
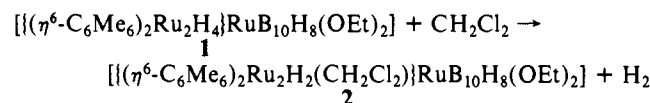


Figure 2. Diagram showing the binding of the dichloromethane molecule to the Ru_3 triangle in $[(\eta^6\text{-C}_6\text{Me}_6)_2\text{Ru}_2\text{H}_2(\text{CH}_2\text{Cl}_2)]\text{RuB}_{10}\text{H}_8(\text{OEt})_2$. Thermal ellipsoids are drawn at the 50% probability level. Selected interatomic distances (angstroms) and angles (degrees) are as follows: Ru(1)-Ru(2), 3.100 (1); Ru(2)-Ru(3), 2.869 (1); Ru(1)-Ru(3), 3.106 (1); Ru(1)-Cl(1), 2.403 (3); Ru(1)-Cl(2), 2.396 (2); Ru(2)-Cl(2), 2.315 (3); Ru(3)-Cl(1), 2.319 (3); Ru(1)-H(12A), 2.19 (8); Ru(2)-H(12A), 1.92 (7); Ru(3)-H(12A), 1.88 (7); Ru(2)-H(12B), 2.20 (7); Ru(3)-H(12B), 2.20 (7); C(31)-Cl(1), 1.803 (9); C(31)-Cl(2), 1.827 (9); Ru(1)-Cl(1)-Ru(3), 82.2 (1); Ru(1)-Cl(2)-Ru(2), 82.3 (1); Cl(1)-C(31)-Cl(2), 102.4 (5). Proton NMR data are as follows: $\delta(^1\text{H})$ (H(1)) +2.49 ppm (d), $\delta(^1\text{H})$ (H(2)) +4.89 ppm (ddd), $\delta(^1\text{H})$ (H(12A)) -14.74 ppm (dd), $\delta(^1\text{H})$ (H(12B)) -22.40 ppm (dd); $^2J(\text{H}(1)\text{-H}(2))$ 10.1 Hz, $^4J(\text{H}(2)\text{-H}(12A))$ 1.2 Hz, $^4J(\text{H}(2)\text{-H}(12B))$ 5.3 Hz, $^2J(\text{H}(12A)\text{-H}(12B))$ 4.9 Hz.

mosphere of dry N_2 for 43 h. Purification was effected by repeated preparative thin-layer chromatography on silica with CH_2Cl_2 as the eluting solvent (green band, $R_f = 0.28$).

The idealized stoichiometry is given by the equation



(4) Bown, M.; Fontaine, X. L. R.; Greenwood, N. N.; MacKinnon, P.; Kennedy, J. D.; Thornton-Pett, M. *J. Chem. Soc., Dalton Trans.* **1987**, 2781.

Compound **2** is an air-stable green solid; crystals suitable for a single-crystal X-ray structure analysis were grown by vapor diffusion of diethyl ether into a dichloromethane solution.

The molecular arrangement determined for **2** is shown in Figure 1 and that of the $\{\text{Ru}_3\text{H}_2(\text{CH}_2\text{Cl}_2)_2\}$ fragment is depicted in Figure 2. The analysis reveals a triangle of ruthenium atoms with two of the metals in coordination with two hexamethylbenzene ligands; the third ruthenium atom forms part of a $\{2,3\text{-(OEt)}_2\text{-isocloso-1-RuB}_{10}\text{H}_8\}$ subcluster. The CH_2Cl_2 occupies a position on one side of the $\{\text{Ru}_3\}$ triangle such that each Cl forms an asymmetric bridge between a pair of ruthenium atoms, notionally replacing the H(1,2) and H(1,3) hydride bridges of the parent molecule.⁴ The ruthenium atom involved in the metallaundecaborane moiety is associated with the longer Ru–Cl distances of 2.403 (3) and 2.396 (2) Å for Ru(1)–Cl(1) and Ru(1)–Cl(2), respectively. These may be compared with the more normal⁵ distances for Ru(2)–Cl(2) and Ru(3)–Cl(1) of 2.315 (3) and 2.319 (3) Å, respectively. Two bridging hydride atoms have been located: H(12A) is approximately equidistant from Ru(2) and Ru(3), and H(12B) is approximately equidistant from all three metal atoms but at a significantly longer distance. The dimensions of the *isocloso*-1-metallaundecaborane are similar to those in **1**⁴ and in related compounds of ruthenium^{6–8} and osmium.⁹ The Ru(1) atom center may be regarded as being formally ruthenium(II) if the hypercloso view^{10–12} is adopted, or ruthenium(IV) for the *isocloso* view.^{6,8,9,13,14} Whichever view is taken, the two hexamethylbenzene ligands contribute six electrons each, the formal borane ligand four, the two bridging hydrogen atoms one each, and the three ruthenium atoms eight each. The chlorine–ruthenium bond lengths suggest that both chlorine atoms are donating two lone pairs to the cluster, thus giving a total cluster electron count of 50, two greater than the 48 usually¹⁵ associated with triangular clusters. The greater thermal stability of **2**, which is stable in refluxing acetonitrile, in comparison with $\text{Ag}_2(\text{CH}_2\text{Cl}_2)_4\text{Pd}(\text{OTeF}_5)_4$,¹ which is stable only below -20°C , may reflect the stronger interaction of the dichloromethane in **2**, where both lone pairs of electrons on each chlorine atom are involved in cluster bonding.

Refluxing **1** in dichloromethane alone, even over an extended period, was shown to effect no change, indicating a role for phenylacetylene in the formation of **2**. A second product, isolated from the reaction in 69% yield (based on Ru), has been characterized as the $\mu\text{-}\eta^2\text{-alkenyl}$ compound¹⁶ $\{[(\eta^6\text{-C}_6\text{Me}_6)_2\text{Ru}_2\text{H}_3(\mu\text{-}\eta^2\text{-HC=CHPh})]\text{RuB}_{10}\text{H}_8(\text{OEt})_2\}$. This latter compound may suggest that **2** is formed via a $\mu\text{-}\eta^2\text{-alkenyl}$ complex, with dichloromethane displacing the $\mu\text{-}\eta^2\text{-alkene}$ ligand as styrene.

Acknowledgment. We thank the Massey University Research Fund for a postdoctoral fellowship (M.B) and the NZ University Grants Committee for funding toward equipment. We are grateful to Drs. J. D. Kennedy and X. L. R. Fontaine of the University of Leeds for NMR spectra.

Supplementary Material Available: Tables of atomic coordinates and thermal parameters for all atoms and bond distances and

angles (10 pages); listing of observed and calculated structure factors for $\{[(\eta^6\text{-C}_6\text{Me}_6)_2\text{Ru}_2\text{H}_2(\text{CH}_2\text{Cl}_2)]\text{RuB}_{10}\text{H}_8(\text{OEt})_2\}$ (11 pages). Ordering information is given on any current masthead page.

Ultraviolet Resonance Raman Spectra of Bacteriorhodopsin in the Light-Adapted and Dark-Adapted States

Issei Harada,* Toshiya Yamagishi, Kiyoshi Uchida, and Hideo Takeuchi

Pharmaceutical Institute, Tohoku University
Aobayama, Sendai 980, Japan

Received June 30, 1989

Ultraviolet resonance Raman (UVRR) spectra of bacteriorhodopsin (bR) in the light-adapted (LA) and dark-adapted (DA) states are reported for the first time. The spectra have provided key information on the structures and environments of aromatic amino acid side chains, in particular Trp and Tyr. Conclusions derived are that (1) some Trp side chains in bR₅₆₈ are located in hydrophobic environments, and the hydrophobicity of the Trp side chains or the number of such Trp side chains increases in bR₅₄₈; (2) the $\text{C}_\beta\text{-C}_\gamma$ torsion angles of most Trp side chains are about $+102^\circ$ or -102° in both bR₅₆₈ and bR₅₄₈; (3) the indole N_1H sites of some Trp in bR₅₆₈ and bR₅₄₈ are strongly H-bonded; and (4) at least one Tyr is present as the anionic form (Tyr^-) in bR₅₆₈, and the number of Tyr^- decreases in bR₅₄₈.

LA-bR consists solely of bR₅₆₈ with *all-trans*-retinal as the visible chromophore while DA-bR is a mixture of bR₅₆₈ and bR₅₄₈, the latter containing 13-*cis*, 15-*cis*-retinal.¹ Figure 1 shows the UVRR spectra of LA-bR and DA-bR excited at 240 nm with an H_2 -Raman-shifted pulsed Nd:YAG laser. The spectra are dominated by the bands arising from 8 Trp and 11 Tyr side chains among which the band at 1617 cm^{-1} is an overlap of those of tyrosyl ν_{8a} and tryptophyl $\text{W}1$.⁴ Parts a and b of Figure 2 are 240-nm excited spectra ($1675\text{--}1500\text{-cm}^{-1}$ region) of bR-Tyr-*d* containing ring-deuteriated Tyr (Tyr-*d*, deuteration being 97% at ϵ and 60% at δ), where $\text{W}1$ (1620 cm^{-1}) is separated from the downshifted ν_{8a} of Tyr-*d* at 1598 cm^{-1} . Figure 2c is a 240-nm spectrum of aqueous Trp. Parts d–g of Figure 2 are 253-nm excited spectra of LA-bR, DA-bR, and aqueous Trp and Tyr[–].

The UVRR spectra of individual aqueous aromatic amino acids have now been established.^{8–10} A pair of Trp bands around 1360

(1) Stockburger, M.; Alshuth, T.; Oesterhelt, D.; Gartner, W. *Advances in Spectroscopy: Spectroscopy of Biological Systems*; Clark, R. J. H., Hester, R. E., Eds.; Wiley: New York, 1986; pp 483–535.

(2) Takeuchi, H.; Harada, I. *Proceedings of 15th Symposium on Biomolecular Structure and Functions*; Sanda, 1988, pp 25–28. The spectra were obtained on a JASCO CT-80D double monochromator (600 grooves/mm, 500-nm blaze, second order, with an interference filter (Acton Research 240-B for 240-nm excitation or CORION solar blind filter SB-300-F for 253-nm excitation)) with the intermediate and exit slits wide open, equipped with a multichannel analyzer (Princeton Instruments, IRY-700 with double MCP). Details will be published elsewhere.

(3) Oesterhelt, D.; Stoekenius, W. *Methods Enzymol.* **1973**, *31A*, 667–678.

(4) Harada, I.; Takeuchi, H. *Advances in Spectroscopy: Spectroscopy of Biological Systems*; Clark, R. J. H., Hester, R. E., Eds.; Wiley: New York, 1986; pp 113–175.

(5) Onishi, H.; McCance, M. E.; Gibbons, N. E. *Can. J. Microbiol.* **1965**, *11*, 365–373.

(6) Kinsey, R. A.; Kintanar, A.; Oldfield, E. *J. Biol. Chem.* **1981**, *256*, 9028–9036.

(7) Matthews, H. R.; Matthews, K. S.; Opella, S. J. *Biochim. Biophys. Acta* **1977**, *497*, 1–13.

(8) Rava, R. P.; Spiro, T. G. *J. Phys. Chem.* **1985**, *89*, 1856–1861.

(9) Asher, S. A.; Ludwig, M.; Johnson, C. R. *J. Am. Chem. Soc.* **1986**, *108*, 3186–3197.

(10) Fodor, S. P. A.; Copeland, R. A.; Grygon, C. A.; Spiro, T. G. *J. Am. Chem. Soc.* **1989**, *111*, 5507–5518.

(5) McCormick, F. B.; Gleason, W. B. *Acta Crystallogr., Sect. C: Cryst. Struct. Commun.* **1988**, *C44*, 603.

(6) Crook, J. E.; Elrington, M.; Greenwood, N. N.; Kennedy, J. D.; Woollins, J. D. *Polyhedron* **1984**, *3*, 901.

(7) Elrington, M.; Greenwood, N. N.; Kennedy, J. D.; Thornton-Pett, M. *J. Chem. Soc., Chem. Commun.* **1984**, 1398.

(8) Crook, J. E.; Elrington, M.; Greenwood, N. N.; Kennedy, J. D.; Thornton-Pett, M.; Woollins, J. D. *J. Chem. Soc., Dalton Trans.* **1985**, 2407.

(9) Elrington, M.; Greenwood, N. N.; Kennedy, J. D.; Thornton-Pett, M. *J. Chem. Soc., Dalton Trans.* **1986**, 2277.

(10) Baker, R. T. *Inorganic Chemistry: Towards the 21st Century*; Chrisholm, M. H., Ed.; ACS Symposium Series 211; American Chemical Society: Washington, DC, 1983; p 341 and references therein.

(11) Baker, R. T. *Inorg. Chem.* **1986**, *25*, 109.

(12) Johnston, R. J.; Mingos, D. M. P. *Inorg. Chem.* **1986**, *25*, 3321.

(13) Fowkes, H.; Greenwood, N. N.; Kennedy, J. D.; Thornton-Pett, M. *J. Chem. Soc., Dalton Trans.* **1985**, 517.

(14) Kennedy, J. D. *Inorg. Chem.* **1986**, *25*, 111.

(15) See, for example: Purcell, K. F.; Kotz, J. C. *Inorganic Chemistry*; W. B. Saunders: Philadelphia, 1977; pp 1035–1036.

(16) Sappa, E.; Tiripicchio, A.; Landredi, A. M. *J. Organomet. Chem.* **1983**, *249*, 391.